IEEE Access
Multidisciplinary | Rapid Review | Open Access Journal

Received May 21, 2018, accepted June 19, 2018, date of publication June 27, 2018, date of current version July 25, 2018.

*Digital Object Identifier 10.1109/ACCESS.2018.2850925*

# Design and Analysis of Punctured Terminated Spatially Coupled Protograph LDPC Codes With Small Coupling Lengths

**ZHAOJIE YANG[1,2], (Student Member, IEEE), YI FANG[1,2], (Member, IEEE), GUOJUN HAN[1], (Senior Member, IEEE), GUOFA CAI[1], (Member, IEEE), AND FRANCIS C. M. LAU[3], (Senior Member, IEEE)**

[1]School of Information Engineering, Guangdong University of Technology, Guangzhou 510006, China
[2]National Mobile Communications Research Laboratory, Southeast University, Nanjing 210096, China
[3]Department of Electronic and Information Engineering, The Hong Kong Polytechnic University, Hong Kong

Corresponding author: Yi Fang (fangyi@gdut.edu.cn)

This work was supported in part by the Hong Kong Scholars Program under Grant G-YZ0H, in part by NSF of China under Grant 61771149, Grant 61471131, Grant 61501126, and Grant 61701121, in part by the open research fund of the National Mobile Communications Research Laboratory, Southeast University, under Grant 2018D02, in part by the NSF of Guangdong Province under Grant 2016A030310337, in part by the Guangdong Province Universities and Colleges Pearl River Scholar Funded Scheme under Grant 2017-ZJ022, in part by the Special Innovation Project of the Education Department of Guangdong Province under Grant 2017KTSCX060, and in part by the Guangdong Innovative Research Team Program under Grant 2014ZT05G157.

**ABSTRACT** Spatially coupled protograph (SC-P) low-density parity-check codes can achieve excellent performance and simple implementation when the coupling length is sufficiently large. However, in the case of small coupling lengths, terminated SC-P (TE-SC-P) codes suffer from relatively weaker decoding thresholds and lower code rates compared with the original protograph codes. To address the above issues, we propose a novel design method to enhance the performance of such TE-SC-P codes. Specifically, we develop a bus-topology-like puncturing rule so as to formulate a new family of SC-P codes, referred to as *punctured TE-SC-P (P-TE-SC-P) codes*. Theoretical analyses and simulation results show that the proposed P-TE-SC-P codes possess significant performance gains over conventional SC-P codes and randomly punctured TE-SC-P *(called RP-TE-SC-P)* codes with relatively higher computational complexity.

**INDEX TERMS** Spatially coupled protograph (SC-P) codes, punctured codes, decoding thresholds, minimum distance, coupling length.

## I. INTRODUCTION

As a type of low-density parity-check (LDPC) convolutional-like codes, spatially coupled (SC) LDPC codes have attracted a great deal of attention in recent years. SC-LDPC codes are constructed by coupling multiple identical LDPC codes into a single coupled chain. Different from conventional LDPC block codes, SC-LDPC codes are able to achieve excellent decoding thresholds [1], [2] and satisfy the minimum distance property [3]. It has been proved in [4] that SC-LDPC codes possess significant performance gains over LDPC block codes.

In particular, a terminated SC-LDPC (TE-SC-LDPC) code can attain a larger threshold improvement with respect to the LDPC block code as the coupling length tends to infinity. In this scenario, both the code rate and degree distribution of a TE-SC-LDPC code can approach those of the corresponding block code. However, when the coupling length is small or moderate, the "termination" operation may lead to non-negligible rate loss. Rate loss is one of the most important issue that limits the applications of TE-SC-LDPC codes in practical communication systems. To address this issue, a randomly puncturing scheme has been introduced to TE-SC-LDPC codes in order to form randomly punctured TE-SC-LDPC (RP-TE-SC-LDPC) codes [5]. This puncturing scheme can increase the code rate of conventional TE-SC-LDPC codes at the cost of degrading performance. Furthermore, incorporating some additional structures into the boundaries of a TE-SC-LDPC code can effectively alleviate the rate loss [6], [7].

In parallel with the TE-SC-LDPC codes, another termination scheme has been developed for SC-LDPC codes and a new type of SC-LDPC codes, called *tail-biting SC-LDPC (TB-SC-LDPC) codes*, has been constructed [3], [8]. Although TB-SC-LDPC codes have the same

code rates as their original LDPC block codes, the former codes have no threshold improvement compared with the latter codes. In [9], an energy shaping scheme, which allows the system allocates different transmission energies to different coded bits, has been proposed to improve the decoding thresholds of TB-SC-LDPC codes. However, it cannot accomplish good performance for short codeword lengths. For this reason, the above energy shaping scheme is rather difficult to satisfy the low-latency requirement of modern communication systems [10]. Moreover, an optimized bit mapping scheme has been conceived to trigger the decoding wave of TB-SC-LDPC codes in bit-interleaved coded modulation (BICM) frameworks [11], [12]. In addition to the advancements of asymptotic (i.e., infinite-length) performance, finite-length performance of SC-LDPC codes has been deeply investigated in recent years [13]. For example, the performance of finite-length SC-LDPC codes in the low and high signal-to-noise (SNR) regions has been discussed and optimized in [14] and [15], respectively.

Inspired by the superiority of protograph architectures, a new type of SC-LDPC codes, referred to as *SC protograph (SC-P) codes*, has been formulated recently [8]. With respect to conventional SC-LDPC codes, SC-P codes not only preserve excellent error performance but also enable extra benefits such as simple representation and ease of analysis [3], [8]. This makes the SC-P codes a more preferable choice for both theoretical research and practical applications. Thanks to the aforementioned advantages, a flurry of research activities have been sparked off to improve the structures of SC-P codes [16]. Although the SC-LDPC and SC-P codes have been intensely studied in recent years, their performance with small coupling lengths is relatively unexplored.

With the above motivation, this paper investigates the design of small-coupling-length SC-P codes over AWGN channels. We develop a two-step design method to construct a new family of SC-P codes, referred to as *punctured TE-SC-P (P-TE-SC-P) codes*. Specifically, the proposed design method comprises a symmetric edge-spreading rule and a bus-topology-like puncturing rule, which guarantees excellent error performance in both low-SNR and high-SNR regions without degrading the code rate. A salient feature of the proposed P-TE-SC-P codes is that they can achieve better decoding thresholds, larger free distances, and identical code rates than the original protograph codes and other SC-P codes. Although our code-design methodology is derived under the infinite-codeword-length assumption, the P-TE-SC-P codes exhibit outstanding bit error rates (BERs) under the finite-length codeword condition (e.g., codewords of 5K and 11K). For example, both the regular and irregular P-TE-SC-P codes are shown to possess more than 0.3 dB and 0.9 dB gains over conventional SC-P codes and RP-TE-SC-P codes, respectively.

The remainder of this paper is organized as follows. Section II reviews the protograph codes and two protograph-based SC-LDPC codes. Section III describes two theoretical-analysis methodologies for SC-P codes. Section IV puts forward the proposed design method for the P-TE-SC-P codes and analyzes the performance of various SC-P codes. Section V gives the simulation results. Finally, Section VI concludes this paper.

## II. PROTOGRAPH-BASED SC-LDPC CODES

In this section, we begin with a brief introduction of protograph LDPC codes in Section II-A. Then, we review the construction of protograph-based SC-LDPC codes based on two fundamental approaches (i.e., termination and tail-biting) in Section II-B and Section II-C, respectively.

### A. PROTOGRAPH LDPC CODES

As a novel class of LDPC codes, protograph LDPC codes have received much research interest in various transmission scenarios since they can produce excellent error performance with relatively low complexity [17], [18]. A protograph, which has been introduced by [19], is a Tanner graph with a relatively small number of nodes. Specifically, A protograph $\mathcal{G} = (\mathcal{V}, \mathcal{C}, \mathcal{E})$ consists of a variable-node (VN) set $\mathcal{V}$, a check-node (CN) set $\mathcal{C}$, and an edge set $\mathcal{E}$. Moreover, the cardinalities of $\mathcal{V}$, $\mathcal{C}$, and $\mathcal{E}$ are equal to $n$, $m$, and $E$, respectively. In a protograph, each edge $e_{i,j} \in \mathcal{E}$ connects a VN $v_j \in \mathcal{V}$ and a CN $c_i \in \mathcal{C}$. Unlike a Tanner graph, parallel edges are allowed in a protograph, but they must be thoroughly eliminated during the expansion procedure. Furthermore, a protograph with $n$ VNs and $m$ CNs can be characterized by a base matrix $\mathbf{B} = (b_{i,j})$ of size $m \times n$, where $b_{i,j}$ denotes the number of edges connecting $c_i$ with $v_j$. An expanded protograph, which corresponds to the protograph code, can be obtained by performing the ''copy-and-permute'' operation on a given protograph. This expanded protograph is referred to as a *derived graph*.

### B. TERMINATED SC-P CODES

#### 1) REGULAR TE-SC-P CODES

A $(d_v, d_c, L)$ coupled chain can be obtained by coupling a sequence of $L$ disjoint $(d_v, d_c)$ regular protographs, where $L$ is the coupling length, $d_v$ and $d_c$ are the VN and CN degrees, respectively. Assuming that each protograph is labeled with a time index $t$, one can connect the edges emanating from the VNs at time $t$ ($t = 0, 1, \ldots, L-1$) to the CNs at times $t, t+1, \ldots, t+w$ according to a specific edge-spreading rule, where $0 < w < L$ is the coupling width. Let $a = \gcd(d_v, d_c)$ be the greatest common divisor of $d_v$ and $d_c$. There exist positive integers $b_c$ and $b_v$ satisfying $d_v = ab_c$ and $d_c = ab_v$. The base matrix of a regular TE-SC-P code is defined as

$$\mathbf{B}^{\mathrm{TE}}_{[0,L-1]} = \begin{bmatrix} \mathbf{B}_0 & & & \\ \mathbf{B}_1 & \mathbf{B}_0 & & \\ \vdots & \mathbf{B}_1 & \ddots & \\ \mathbf{B}_w & \vdots & \ddots & \mathbf{B}_0 \\ & \mathbf{B}_w & & \mathbf{B}_1 \\ & & \ddots & \vdots \\ & & & \mathbf{B}_w \end{bmatrix}, \tag{1}$$

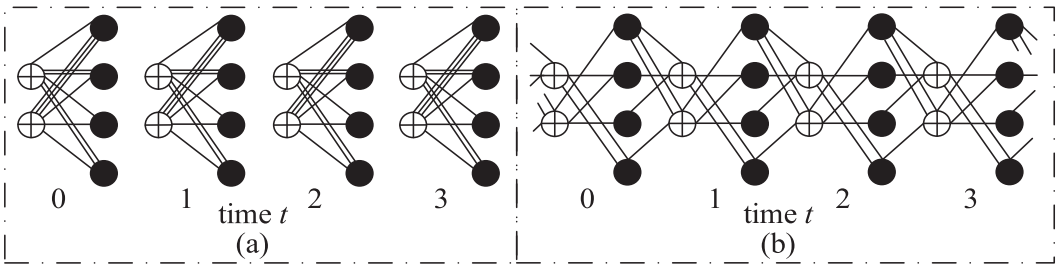


**FIGURE 1.** (a) A sequence of identical, disjoint RJA protographs, and (b) a RJA SC protograph with coupling width $w = 1$.

where $w = a - 1$, and $\mathbf{B}_0, \mathbf{B}_1, \ldots, \mathbf{B}_w$ are identical $b_c \times b_v$ all-one submatrices. In consequence, the size of $\mathbf{B}^{\mathrm{TE}}_{[0,L-1]}$ equals $b_c(L + w) \times Lb_v$.

#### 2) IRREGULAR TE-SC-P CODES

If $\gcd(d_v, d_c) = 1$, the SC-P codes cannot be constructed by the above method. In this situation, the $w + 1$ submatrices $\mathbf{B}_0, \mathbf{B}_1, \ldots, \mathbf{B}_w$ should be constructed from the base matrix $\mathbf{B}$ of an irregular protograph code. The relationship between the submatrices and base matrix is governed by $\sum_{\mu=0}^{w} \mathbf{B}_\mu = \mathbf{B}$, where all matrices share the same size. As an example, Fig. 1 shows the protographs of a repeat-jagged-accumulate (RJA) code and its corresponding SC code, where the VNs and CNs are represented by filled circles and circles with a plus sign, respectively. As can be observed, the base matrix $\mathbf{B}^{\mathrm{RJA}}$ of the RJA code is divided into two submatrices $\mathbf{B}^{\mathrm{RJA}}_0$ and $\mathbf{B}^{\mathrm{RJA}}_1$, which are given as [3]

$$\mathbf{B}^{\mathrm{RJA}} = \begin{bmatrix} 1 & 2 & 1 & 2 \\ 3 & 1 & 1 & 1 \end{bmatrix},$$
$$\mathbf{B}^{\mathrm{RJA}}_0 = \begin{bmatrix} 0 & 1 & 0 & 2 \\ 1 & 1 & 1 & 0 \end{bmatrix}, \quad \mathbf{B}^{\mathrm{RJA}}_1 = \begin{bmatrix} 1 & 1 & 1 & 0 \\ 2 & 0 & 0 & 1 \end{bmatrix}. \tag{2}$$

### C. TAIL-BITING SC-P CODES

The TB-SC-P codes can be constructed from the TE-SC-P codes by combining the CNs at times $t = L, L + 1, \ldots, L + w - 1$ with the corresponding CNs of the same type at times $t = 0, 1, \ldots, w - 1$, respectively. Thus, the base matrix of a TB-SC-P code can be expressed by

$$\mathbf{B}^{\mathrm{TB}}_{[0,L-1]} = \begin{bmatrix} \mathbf{B}_0 & & & \mathbf{B}_w & \cdots & \mathbf{B}_1 \\ \vdots & \ddots & & & \ddots & \vdots \\ \mathbf{B}_{w-1} & & & & & \mathbf{B}_w \\ \mathbf{B}_w & & \mathbf{B}_0 & & & \\ & \ddots & \vdots & \mathbf{B}_0 & & \\ & \ddots & \mathbf{B}_{w-1} & \vdots & \ddots & \\ & & \mathbf{B}_w & \mathbf{B}_{w-1} & \cdots & \mathbf{B}_0 \end{bmatrix}. \tag{3}$$

According to (1) and (3), the base matrix $\mathbf{B}^{\mathrm{TB}}_{[0,L-1]}$ can be constructed from the base matrix $\mathbf{B}^{\mathrm{TE}}_{[0,L-1]}$ by means of adding its last $wb_c$ rows to the first $wb_c$ rows, where the $b_c$ is the number of CNs in each submatrix. As a result, the TB-SC-P codes have the same code rate and degree distribution as their corresponding protograph codes.

## III. THEORETICAL-ANALYSIS METHODOLOGY FOR SC-P CODES

In order to facilitate the design of SC-P codes, the protograph extrinsic information transfer (PEXIT) algorithm and asymptotic distance distribution (ADD) analysis have been proposed in [3], [8], and [20], respectively. In this section, we describe these two theoretical-analysis tools for SC-P codes.

### A. PEXIT ALGORITHM

The EXIT function is of particular importance to trace the convergence of iterative decoding schemes. In [20], the PEXIT algorithm has been proposed to evaluate the decoding thresholds of the protograph codes under belief-propagation (BP) decoding algorithm. This algorithm is also very effective for SC-P codes.

Let $L$ be the log-likelihood-ratio (LLR) of the received signal corresponding to the coded bit over AWGN channels. Then, the mutual information between the coded bit and its corresponding LLR value $L \sim N(\frac{\sigma^2_{\mathrm{ch}}}{2}, \sigma^2_{\mathrm{ch}})$ is denoted by $J(\sigma_{\mathrm{ch}})$, which can be expressed as

$$J(\sigma_{\mathrm{ch}}) = 1 - \int_{-\infty}^{+\infty} \frac{\exp\left(-\frac{(\mu - \sigma^2_{\mathrm{ch}}/2)^2}{2\sigma^2_{\mathrm{ch}}}\right)}{\sqrt{2\pi\sigma^2_{\mathrm{ch}}}} \times \log_2[1 + \exp(-\mu)]\, \mathrm{d}\mu. \tag{4}$$

The derivation of $J(\cdot)$ and its inverse function $J^{-1}(\cdot)$ can be obtained in [21].

In order to illustrate the process of the algorithm, we define five different notations of mutual information for the SC-P codes as follows.

- $I_{\mathrm{AV}}(i, j)$ denotes the *a prior* mutual information from the CN $c_i$ to the VN $v_j$.
- $I_{\mathrm{AC}}(i, j)$ denotes the *a prior* mutual information from the VN $v_i$ to the CN $c_j$.

- $I_{EV}(i,j)$ denotes the *extrinsic* mutual information from the VN $v_i$ to the CN $c_j$.
- $I_{EC}(i,j)$ denotes the *extrinsic* mutual information from the CN $c_i$ to the VN $v_j$.
- $I_{APP}(j)$ denotes the *a posteriori* mutual information of a VN $v_j$.

In addition, we assume that the maximum number of iterations in the algorithm is $T_{\max}$. Besides, we have $I_{AC}(i,j) = I_{EV}(i,j)$ and $I_{AV}(i,j) = I_{EC}(i,j)$ in each iteration. Thus, based on the above definitions, the PEXIT algorithm over an AWGN channel can be described as follows.

1) **Initialization:** For $i = 1, 2, \ldots, m$ and $j = 1, 2, \ldots, n$, initialize $I_{AV}(i,j) = 0$. Then, compute the variance of the channel initial LLR as $\sigma^2_{ch,j} = 8R(E_b/N_0)$, where $R$ is the code rate, and $E_b/N_0$ is the SNR per bit. As a special case, $\sigma^2_{ch,j} = 0$ if the $j$-th VN $v_j$ is punctured.
2) **Updating VN-to-CN mutual information:** For $i = 1, 2, \ldots, m$ and $j = 1, 2, \ldots, n$, the *extrinsic* mutual information sent from the VN $v_i$ to the CN $c_j$ can be calculated by

$$I_{EV}(i,j) = J\left(\left(\sum_{s\neq i} b_{s,j}[J^{-1}(I_{AV}(s,j))]^2 + (b_{i,j}-1)[J^{-1}(I_{AV}(i,j))]^2 + \sigma^2_{ch,j}\right)^{1/2}\right). \tag{5}$$

3) **Updating CN-to-VN mutual information:** For $i = 1, 2, \ldots, m$ and $j = 1, 2, \ldots, n$, the *extrinsic* mutual information sent from the CN $c_i$ to the VN $v_j$ can be measured as

$$I_{EC}(i,j) = 1 - J\left(\left(\sum_{s\neq j} b_{i,s}[J^{-1}(1-I_{AC}(i,s))]^2 + (b_{i,j}-1)[J^{-1}(1-I_{AC}(i,j))]^2\right)^{1/2}\right). \tag{6}$$

4) **Computing the a posteriori mutual information of VNs:** For $j = 1, 2, \ldots, n$, the *a posteriori* mutual information of $V_j$ can be calculated by

$$I_{APP}(j) = J\left(\left(\sum_{i=1}^{m} b_{i,j}[J^{-1}(I_{AV}(i,j))]^2 + \sigma^2_{ch,j}\right)^{1/2}\right). \tag{7}$$

5) **Finalization:** If the *a posteriori* mutual information values $I_{APP}(j) = 1$ for all $j = 1, 2, \ldots, n$, the corresponding $E_b/N_0$ is considered as the decoding threshold of the code and the iterative process is terminated; otherwise, repeat Steps 2)-4) continuously.

According to the PEXIT algorithm, the decoding threshold is the smallest $E_b/N_0$ (dB) that guarantees the *a posteriori* mutual information of all VNs in an SC-P code converging to the value of unity.

### B. ADD ANALYSIS

The PEXIT algorithm can be exploited to design the SC-P codes with capacity-approaching thresholds. Although the SC-P codes optimized by the PEXIT algorithm can exhibit good performance in the low-SNR region, they may suffer from an error floor in the high-SNR region, especially in moderate or short codeword-length cases [17]. Therefore, how to analyze and optimize the performance of such codes in the high-SNR region is a critical issue.

Litsyn and Shevelev [22] have pointed out that the minimum distance of the codewords can reflect the error performance in the high-SNR region. For protograph codes, the minimum (Hamming) distance, i.e., $d_{\min}$, can be evaluated by $N' \times \delta_{\min}$, where $N'$ and $\delta_{\min}$ are the codeword length and the typical minimum distance ratio (TMDR). According to the value of $\delta_{min}$, we can determine whether the $d_{\min}$ grows linearly with the codeword length (i.e., the linear-minimum-distance property holds). In summary, a protograph code having a larger $\delta_{\min}$ can achieve relatively better error performance in the high-SNR region [23].

In contrast to conventional protograph codes, the minimum (free) distance (i.e., $d_{free}$), instead of the minimum Hamming distance, are used to characterize the high-SNR error performance of SC protograph codes due to the introduction of constraint length. For such type of codes, the linear-minimum-distance property for SC-P codes is defined as the phenomenon that the $d_{free}$ grows linearly with the constraint length [24], i.e.,

$$d_{free} = \delta_{free}\nu_s, \tag{8}$$

where $\delta_{free}$ is the free distance growth rate and $\nu_s$ is the constraint length. As a consequence, an SC-P code with a large $\delta_{free}$ should possess excellent error performance and low error floor in the high-SNR region. Mitchell *et al.* [8] have pointed out that the scaled growth rates $\delta^{(L)}_{\min}L/(w+1)$ of the SC-P codes will converge to a fixed value (i.e., a bound on the $\delta_{free}$ of the SC-P codes) as $L$ increases. Therefore, this parameter can be approximately expressed by

$$\delta^{(L)}_{free} \approx (\delta^{(L)}_{\min}L)/(w+1), \tag{9}$$

where $\delta^{(L)}_{\min}$ is the TMDR of the SC-P codes with a coupling length $L$. As proved in [3], an SC-P code having a larger $\delta^{(L)}_{free}$ should exhibit a higher free distance and better performance in the high-SNR region.

Based on the above discussion, an SC-P code, which not only has a small decoding threshold but also has a large free distance growth rate, should achieve excellent error performance in both low and high-SNR regions.

## IV. DESIGN AND ANALYSIS OF PROPOSED P-TE-SC-P CODES

### A. PROPOSED DESIGN METHOD

The base matrix of a regular TE-SC-P code satisfies a symmetric property from the perspective of CN degrees. In particular, the CNs at the two ends of the base matrix possess

a reduced number of degrees compared with the CNs at the middle of the base matrix. These lower-degree CNs always pass more reliable messages to their associated VNs, which may improve the decoding threshold. Moreover, punctured VNs can be incorporate into TE-SC-P codes to compensate the code-rate loss. Although the puncturing technique was usually exploited to increase the code rate at the price of sacrificing error performance [17], it was demonstrated that the performance of protograph codes can also be enhanced if the punctured VNs are properly selected. This property also holds for SC-P codes.

Based on the above discussion and assuming a rate-$R^{\mathrm{P}}$ protograph code with a $b_c \times b_v$ protograph, a two-step design method is conceived for P-TE-SC-P codes as follows.

#### 1) SYMMETRIC EDGE SPREADING

With an aim to offsetting the rate loss of TE-SC-P code with the fewest punctured VNs, the base matrix of a protograph is divided into two submatrices (i.e., $w = 1$). Thus, lowest decoding complexity will be increased in the construction of P-TE-SC-P codes. Specifically, the elements larger than 1 in the base matrix are decomposed into the two submatrices in a quasi-uniform manner. Then, the remaining elements of "1" are properly assigned to the two submatrices so as to make the weights of their respective columns (i.e., degrees of their respective VNs) as identical as possible. The resultant TE-SC-P code is called *improved TE-SC-P (ITE-SC-P) code*. Note that the submatrices obtained in the above method are not unique.

#### 2) BUS-TOPOLOGY-LIKE PUNCTURING

With an aim to addressing the rate-loss problem caused by the "termination" operation, punctured bit(s) is/are incorporated into the ITE-SC-P codes. In particular, the first punctured VN should be added to connect to all CNs (i.e., connection structure between this punctured VN and all CNs is analogous to a bus topology). Precisely speaking, this punctured VN has two (parallel) edges connecting to the $(2j' - 1)$-th CN and has a single edge connecting to the $(2j')$-th CN, where $j' = 1, 2, \ldots, \frac{b_c(L+w)}{2}$. If the code rate of the new SC-P code $R_L^{\text{P-TE}}$ is still smaller than $R^{\mathrm{P}}$, some additional degree-2 punctured VNs should be introduced to the existing SC-P code until $R_L^{\text{P-TE}} = R^{\mathrm{P}}$. In doing so, these punctured VNs are properly connected to the first and last $b_c \times w$ CNs so as to satisfy the CN-degree symmetric property at the two ends of the base matrix. The rate-$R^{\mathrm{P}}$ ITE-SC-P code with punctured VNs is referred to as *P-TE-SC-P* code. As a consequence, the size of a P-TE-SC-P code equals $b_c(L + w) \times (b_v L + n_{\mathrm{p}})$, where $n_{\mathrm{p}}$ is the number of punctured VNs.

Following the proposed design method, we will demonstrate that we can construct the P-TE-SC-P codes that possess excellent performance over AWGN channels, especially for small values of $L$. As an example, we show the structures of two P-TE-SC-P codes constructed from the rate-1/2 (3, 6) protograph code and RJA protograph code as below.

*Example 1:* Given a rate-1/2 (3, 6) protograph code, one can divide its base matrix $\mathbf{B}^{(3,6)}$ into two submatrices, i.e., $\mathbf{B}_0^{(3,6)'}$ and $\mathbf{B}_1^{(3,6)'}$, exploiting the edge-spreading rule, where

$$\mathbf{B}^{(3,6)} = \begin{bmatrix} 3 & 3 \end{bmatrix}, \quad \mathbf{B}_0^{(3,6)'} = \begin{bmatrix} 1 & 2 \end{bmatrix}, \quad \mathbf{B}_1^{(3,6)'} = \begin{bmatrix} 2 & 1 \end{bmatrix}. \tag{10}$$

Then, a (3, 6) ITE-SC-P code can be formulated by substituting $\mathbf{B}_0^{(3,6)'}$ and $\mathbf{B}_1^{(3,6)'}$ into (1). Furthermore, a punctured VN is added into the (3, 6) ITE-SC-P code in accordance with the bus-topology-like puncturing rule so as to construct a rate-1/2 (3, 6) P-TE-SC-P code. The base matrix of the (3, 6) P-TE-SC-P code with a coupling length $L = 12$ is expressed by

$$\mathbf{B}_{[0,11]}^{\text{P-TE-(3,6)}} = \begin{bmatrix} 1 & 2 & & & & & & & & & & 2 \\ 2 & 1 & 1 & 2 & & & & & & & & 1 \\ & & 2 & 1 & 1 & 2 & & & & & & 2 \\ & & & & 2 & 1 & & & & & & 1 \\ & & & & & & \ddots & & & & & \vdots \\ & & & & & & \ddots & 1 & 2 & & & 2 \\ & & & & & & & 2 & 1 & 1 & 2 & 1 \\ & & & & & & & & & 2 & 1 & 2 \end{bmatrix}, \tag{11}$$

where the size of this base matrix is $13 \times 25$, and the last column corresponds to the punctured VN.

*Example 2:* Following the similar steps as in *Example 1*, one can also obtain two improved submatrices corresponding to a rate-1/2 RJA code (i.e., (2)), which are shown as

$$\mathbf{B}_0^{\text{RJA'}} = \begin{bmatrix} 0 & 1 & 0 & 1 \\ 2 & 0 & 1 & 1 \end{bmatrix}, \quad \mathbf{B}_1^{\text{RJA'}} = \begin{bmatrix} 1 & 1 & 1 & 1 \\ 1 & 1 & 0 & 0 \end{bmatrix}. \tag{12}$$

Thus, the base matrix of a rate-1/2 RJA P-TE-SC-P code with a coupling length $L = 6$ can be described as

$$\mathbf{B}_{[0,5]}^{\text{P-TE-RJA}} = \begin{bmatrix} 0 & 1 & 0 & 1 & & & & & & & 2 & 0 \\ 2 & 0 & 1 & 1 & & & & & & & 1 & 1 \\ 1 & 1 & 1 & 1 & 0 & 1 & 0 & 1 & & & 2 & 0 \\ 1 & 1 & 0 & 0 & 2 & 0 & 1 & 1 & & & 1 & 0 \\ & & & & 1 & 1 & 1 & 1 & & & 2 & 0 \\ & & & & 1 & 1 & 0 & 0 & & & 1 & 0 \\ & & & & & & & & \ddots & & \vdots & \vdots \\ & & & & & & & & 0 & 1 & 2 & 0 \\ & & & & & & & & 2 & 0 & 1 & 1 \\ & & & & & & & & 1 & 1 & 2 & 0 \\ & & & & & & & & 1 & 1 & 1 & 1 \end{bmatrix}, \tag{13}$$

where the size of this base matrix is $14 \times 26$, and the last two columns correspond to the punctured VNs.

**TABLE 1. Code rates of the (3, 6) SC-P codes and RJA SC-P codes with three different coupling methods. The coupling lengths of (3, 6) SC-P codes and RJA SC-P codes are 12 and 6, respectively.**

| Code Type \ Coupling Method | TE-SC-P | TB-SC-P | P-TE-SC-P |
|---|---|---|---|
| $(3,6)$ protograph code | $5/12$ | $1/2$ | $1/2$ |
| RJA protograph code | $5/12$ | $1/2$ | $1/2$ |

To verify the superiority of our proposed P-TE-SC-P codes, codes including (3, 6) TE-SC-P code, (3, 6) TB-SC-P code, original (3, 6) protograph code, RJA TE-SC-P code, RJA TB-SC-P code, and original RJA protograph code in [3] are used as benchmarks in the forthcoming performance analyses.

### B. CODE-RATE ANALYSIS

#### 1) TE-SC-P CODES

For a finite coupling length $L$, the code rate of a TE-SC-P code can be measured as

$$R_L^{\mathrm{TE}} = 1 - \frac{n_c}{n_v} = 1 - \frac{(L+w)b_c}{Lb_v} = 1 - \left(\frac{L+w}{L}\right)(1-R^{\mathrm{P}}), \tag{14}$$

where $n_c$ and $n_v$ are the numbers of CNs and transmitted VNs in its base matrix, respectively. Moreover, $R^{\mathrm{P}} = 1 - b_c/b_v$ is the code rate of its original protograph code containing $b_c$ CNs and $b_v$ VNs.

#### 2) TB-SC-P CODES

The code rate of a TB-SC-P code is the same as that of its corresponding protograph code, which can be derived as

$$R_L^{\mathrm{TB}} = 1 - \frac{Lb_c}{Lb_v} = 1 - b_c/b_v = R^{\mathrm{P}}. \tag{15}$$

#### 3) P-TE-SC-P CODES

According to the proposed design method in Sect. III-A, the code rate of a P-TE-SC-P code is

$$R_L^{\text{P-TE}} = (n_v - n_c + n_p)/n_v = R_L^{\mathrm{TE}} + n_p/n_v > R_L^{\mathrm{TE}}. \tag{16}$$

As can be observed, the code rate of a P-TE-SC-P code not only is higher than $R_L^{\mathrm{TE}}$, but also can reach $R^{\mathrm{P}}$ by varying the value of $n_p$. For instance, Table 1 shows the code rates of the (3, 6) SC-P codes and RJA SC-P codes with three different coupling methods. As illustrated, both the P-TE-SC-P codes and TB-SC-P codes achieve a rate of $1/2$, while the TE-SC-P codes only accomplish a rate of $5/12$.

### C. ASYMPTOTIC-PERFORMANCE ANALYSIS

In this subsection, we analyze decoding thresholds and free distance growth rates of the proposed P-TE-SC-P codes by exploiting the PEXIT and ADD algorithms mentioned in Sect. III in order to validate their performance superiority.

#### 1) DECODING THRESHOLD

We estimate the decoding thresholds of (i) the three (3, 6) SC-P codes, (ii) the original (3, 6) protograph code, (iii) the three RJA SC-P codes, and (iv) the original RJA protograph code, by exploiting the PEXIT algorithm, and present the results in Table 2. Referring to this table, the P-TE-SC-P codes exhibit the smallest decoding thresholds among all SC-P codes and original protograph codes. Considering the (3, 6) protograph, the mutual information of proposed P-TE-SC-P code can converge to the value of unity at $E_b/N_0 = 0.5$ dB, while the TB-SC-P code and TE-SC-P code require much larger SNRs (i.e., $E_b/N_0 > 1.1$ dB) to do so. This implies that the P-TE-SC-P codes can achieve the best error performance in the low-SNR region.

**TABLE 2. Decoding thresholds of the original protograph code and the SC-P codes over an AWGN channel. The coupling lengths of (3, 6) SC-P codes and RJA SC-P codes are 12 and 6, respectively.**

| $(3,6)$ Codes | protograph | TE-SC-P | TB-SC-P | P-TE-SC-P |
|---|---|---|---|---|
| $(E_b/N_0)_{\mathrm{th}}$/dB | 1.103 | 1.115 | 1.103 | 0.500 |
| RJA Codes | protograph | TE-SC-P | TB-SC-P | P-TE-SC-P |
| $(E_b/N_0)_{\mathrm{th}}$/dB | 1.001 | 1.075 | 1.001 | 0.649 |

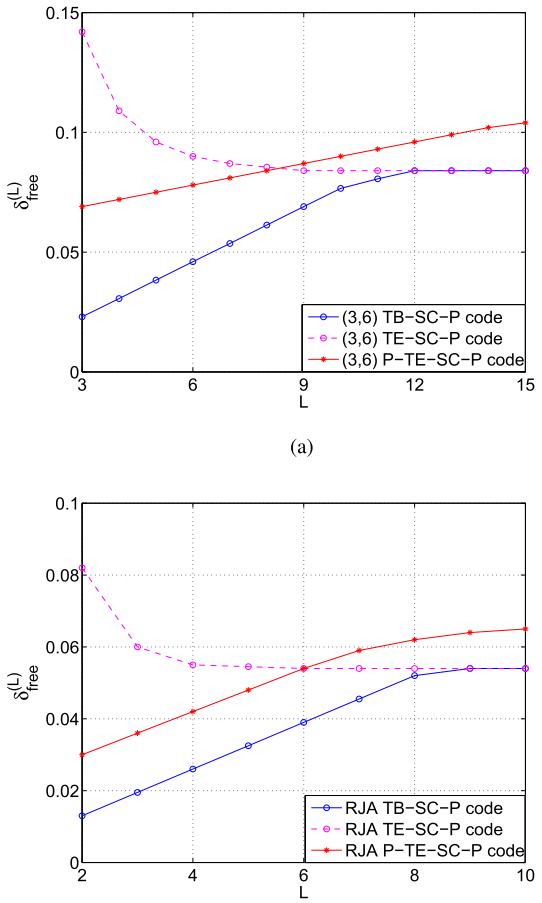


**FIGURE 2. Free distance growth rates of (a) three (3, 6) SC-P codes and (b) three RJA SC-P codes.**

#### 2) FREE DISTANCE GROWTH RATE

As a further insight, we analyze the $\delta_{\mathrm{free}}^{(L)}$ of the aforementioned SC-P codes and show the results in Fig. 2. As observed

**TABLE 3. Number of operations required for CN update within each iteration.**

| Algorithm | Addition | Multiplication |
|---|---|---|
| BP | $3N\overline{d}_v$ | $\sum_{i=1}^{M} d_{c_i}^2 - \overline{d}_c M$ |

**TABLE 4. Number of operations required for CN update of the (3, 6) SC-P codes and RJA SC-P codes within each iteration. The codeword length is 4800, the coupling lengths of (3, 6) SC-P codes and RJA SC-P codes are 12 and 6, respectively.**

| Code Type | Addition | Multiplication |
|---|---|---|
| $(3, 6)$ TE-SC-P Code | $4.320 \times 10^4$ | $6.560 \times 10^4$ |
| $(3, 6)$ TB-SC-P Code | $4.320 \times 10^4$ | $7.200 \times 10^4$ |
| $(3, 6)$ P-TE-SC-P Code | $5.520 \times 10^4$ | $1.144 \times 10^5$ |
| RJA TE-SC-P Code | $4.320 \times 10^4$ | $6.560 \times 10^4$ |
| RJA TB-SC-P Code | $4.320 \times 10^4$ | $7.200 \times 10^4$ |
| RJA P-TE-SC-P Code | $5.700 \times 10^4$ | $1.148 \times 10^5$ |

from Fig. 2(a), it is apparent that the (3, 6) P-TE-SC-P code has a larger $\delta_{\text{free}}^{(L)}$ than its corresponding TE-SC-P code and TB-SC-P code when $L \geq 9$. Moreover, with an increasing $L$, the $\delta_{\text{free}}^{(L)}$ of both TB-SC-P code and TE-SC-P code converge to a constant, while that of the P-TE-SC-P code continues to increase. Hence, the P-TE-SC-P codes should outperform the other two SC-P codes in the high-SNR region. For the RJA SC-P codes, similar conclusions can be drawn from Fig. 2(b).

### D. COMPUTATIONAL COMPLEXITY ANALYSIS

During the LDPC decoding process, the computational complexity for CN update within each iteration determines the overall decoding complexity. Therefore, based on the BP algorithm, we evaluate the number of operations required in each iteration. The results are shown in Table 3, where $N$ and $M$ are the number of transmitted VNs and CNs, respectively; $d_{c_i}$ is the degree of the $i$th CN; $\overline{d}_v$ and $\overline{d}_c$ are the average degrees of VNs and CNs; More specifically, we illustrate the computational complexities of the (3, 6) SC-P codes and RJA SC-P codes with $N = 4800$ in Table 4. As can be seen from this table, the proposed P-TE-SC-P codes have relatively higher computational complexity than the TE-SC-P and TB-SC-P codes because incorporating the additional VNs leads to a higher averaged degree.

## V. SIMULATION RESULTS

Based on the different coupling methods, we present some simulation results of the (3, 6) SC-P codes and RJA SC-P codes with a code rate $R = 1/2$ over AWGN channels. In particular, the transmitted codeword lengths (excluding the punctured bits) are assumed to be $N = 4800$ and $N = 10800$. Furthermore, all codewords are decoded with BP algorithm and the maximum number of BP iterations equals $T = 100$.

### A. BER PERFORMANCE COMPARISON BETWEEN THE PROPOSED P-TE-SC-P CODES AND CONVENTIONAL SC-P CODES

Fig. 3 depicts the BER curves of the original (3, 6) protograph code, TE-SC-P code, TB-SC-P code, and the proposed (3, 6) P-TE-SC-P code. Referring to the figure, for $N = 4800$, the proposed P-TE-SC-P code is significantly superior to the TB-SC-P code, which further outperforms the original protograph code, and TE-SC-P code. Especially, the proposed P-TE-SC-P code and TE-SC-P code are the best-performing and worst-performing codes, respectively. For example, at a BER of $10^{-5}$, the proposed P-TE-SC-P code achieves a gain of about 0.3 dB over the TB-SC-P code, while the TB-SC-P code has additional gains of about 0.1 dB over the TE-SC-P code. Furthermore, at $E_b/N_0 = 1.4$ dB, the proposed P-TE-SC-P code achieves a BERs of $9 \times 10^{-6}$, while the TB-SC-P code and TE-SC-P code only accomplish BERs of $2 \times 10^{-3}$, $5 \times 10^{-3}$, respectively. It is noteworthy that the P-TE-SC-P code does not have the error-floor phenomena when the BER equals $1.5 \times 10^{-6}$. From this perspective, a larger gain can be expected at a lower BER. More importantly, the performance advantage of the proposed (3, 6) P-TE-SC-P code can be preserved when the codeword length is increased to $N = 10800$. Similar observations can be also found in the results for the proposed RJA P-TE-SC-P code (see Fig. 4).

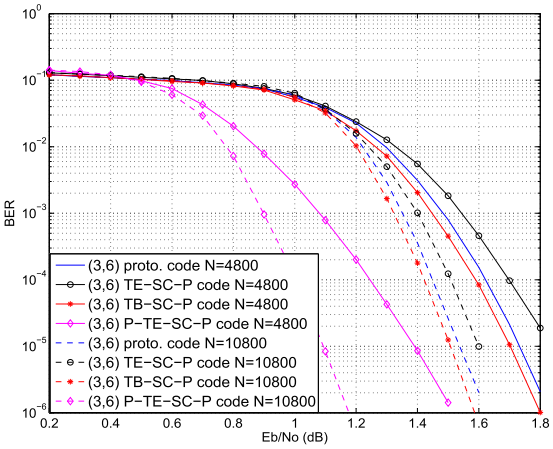


**FIGURE 3. BER curves of the original (3, 6) protograph code, (3, 6) TE-SC-P code, (3, 6) TB-SC-P code, and (3, 6) P-TE-SC-P code. The coupling length for all (3, 6) SC-P codes is 12.**

### B. BER PERFORMANCE COMPARISON BETWEEN THE PROPOSED PUNCTURING SCHEME AND THE RANDOMLY PUNCTURING SCHEME

The BER performance curves of the (3, 6) P-TE-SC-P code and RP-TE-SC-P code [5] (i.e., the proposed puncturing scheme and the randomly puncturing scheme [5]) are depicted in Fig. 5. As can be observed, the error performance of the proposed P-TE-SC-P code is much better than the RP-TE-SC-P code in [5]. Specifically, for $N = 4800$, the proposed P-TE-SC-P code obtains a gain of about 0.9 dB over the RP-TE-SC-P code at a BER of $1 \times 10^{-5}$. In addition, at $E_b/N_0 = 1.5$ dB, the proposed P-TE-SC-P code achieves a desirable BER of $1.5 \times 10^{-6}$, while the RP-TE-SC-P code only accomplishes a BER of $5 \times 10^{-2}$. Moreover, the trend of the BER performance curves for the case of $N = 10800$ is highly consistent with that of $N = 4800$. Based on the RJA

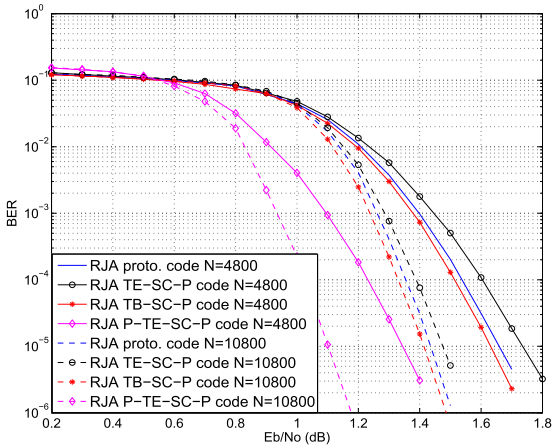


**FIGURE 4.** BER curves of the original RJA protograph code, RJA TE-SC-P code, RJA TB-SC-P code, and RJA P-TE-SC-P code. The coupling length for all RJA SC-P codes is 6.

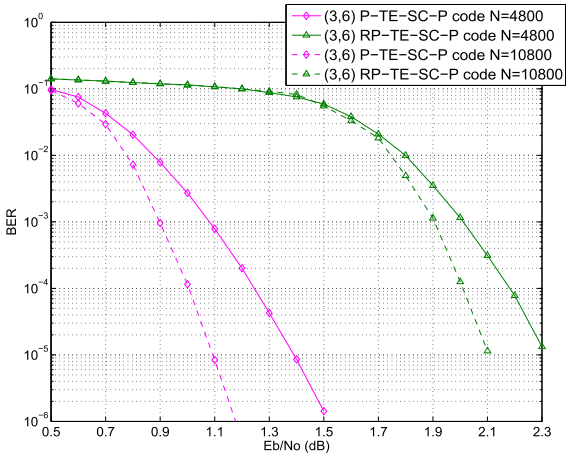


**FIGURE 5.** BER curves of the (3, 6) P-TE-SC-P code and RP-TE-SC-P code. The coupling length is 12.

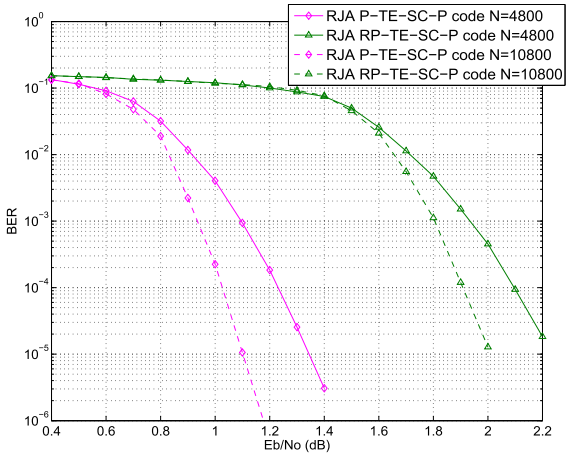


**FIGURE 6.** BER curves of the RJA P-TE-SC-P code and RP-TE-SC-P code. The coupling length is 6.

protograph, the TE-SC-P code with the proposed puncturing scheme still outperforms the counterpart with the randomly puncturing scheme (see Fig. 6), which further demonstrates the superiority of our design.

Besides, we have carried out simulations for different values of $L$, and have found that the proposed P-TE-SC-P codes always outperform the other three types of SC-P codes.

## VI. CONCLUSIONS

In this paper, we have conceived a novel design method to construct a new family of SC-P codes with small coupling lengths, called *P-TE-SC-P codes*. The proposed design method includes two steps, i.e., symmetric edge spreading and bus-topology-like puncturing, which not only can ensure desirable decoding threshold and free distance growth rate, but also can avoid code-rate loss. Theoretical analyses and BER simulations have indicated that the proposed P-TE-SC-P codes have much better performance compared with the corresponding TB-SC-P, TE-SC-P, RP-TE-SC-P, and original protograph codes at the cost of relatively higher computational complexity. Thanks to the excellent performance, the family of P-TE-SC-P codes appear to be a good candidate for practical use in future wireless communication systems.

## REFERENCES

[1] S. Kudekar, T. J. Richardson, and R. L. Urbanke, "Spatially coupled ensembles universally achieve capacity under belief propagation," *IEEE Trans. Inf. Theory*, vol. 59, no. 12, pp. 7761–7813, Dec. 2013.
[2] M. Lentmaier, A. Sridharan, D. J. Costello, and K. S. Zigangirov, "Iterative decoding threshold analysis for LDPC convolutional codes," *IEEE Trans. Inf. Theory*, vol. 56, no. 10, pp. 5274–5289, Oct. 2010.
[3] D. G. M. Mitchell, A. E. Pusane, and D. J. Costello, Jr., "Minimum distance and trapping set analysis of protograph-based LDPC convolutional codes," *IEEE Trans. Inf. Theory*, vol. 59, no. 1, pp. 254–281, Jan. 2013.
[4] A. E. Pusane, R. Smarandache, P. O. Vontobel, and D. J. Costello, "Deriving good LDPC convolutional codes from LDPC block codes," *IEEE Trans. Inf. Theory*, vol. 57, no. 2, pp. 835–857, Feb. 2011.
[5] D. G. M. Mitchell, M. Lentmaier, A. E. Pusane, and D. J. Costello, "Randomly punctured LDPC codes," *IEEE J. Sel. Areas Commun.*, vol. 34, no. 2, pp. 408–421, Feb. 2016.
[6] K. Tazoe, K. Kasai, and K. Sakaniwa, "Efficient termination of spatially-coupled codes," in *Proc. ITW*, Sep. 2012, pp. 30–34.
[7] M. R. Sanatkar and H. D. Pfister, "Increasing the rate of spatially-coupled codes via optimized irregular termination," in *Proc. ISTC*, Sep. 2016, pp. 31–35.
[8] D. G. M. Mitchell, M. Lentmaier, and D. J. Costello, "Spatially coupled LDPC codes constructed from protographs," *IEEE Trans. Inf. Theory*, vol. 61, no. 9, pp. 4866–4889, Sep. 2015.
[9] T. Jerkovits, G. Liva, and A. G. I. Amat, "Improving the decoding threshold of tailbiting spatially coupled LDPC codes by energy shaping," *IEEE Commun. Lett.*, vol. 22, no. 4, pp. 660–663, Feb. 2018.
[10] J. Wen, B. Zhou, W. H. Mow, and X.-W. Chang, "An efficient algorithm for optimally solving a shortest vector problem in compute-and-forward design," *IEEE Trans. Wireless Commun.*, vol. 15, no. 10, pp. 6541–6555, Oct. 2016.
[11] S. Cammerer, V. Aref, L. Schmalen, and S. ten Brink, "Triggering wave-like convergence of tail-biting spatially coupled LDPC codes," in *Proc. 50th Annu. Conf. Inf. Sci. Syst. (CISS)*, Mar. 2016, pp. 93–98.
[12] C. Häger, A. G. I. Amat, F. Brännström, A. Alvarado, and E. Agrell, "Terminated and tailbiting spatially coupled codes with optimized bit mappings for spectrally efficient fiber-optical systems," *J. Lightw. Technol.*, vol. 33, no. 7, pp. 1275–1285, Apr. 1, 2015.
[13] P. M. Olmos and R. L. Urbanke, "A scaling law to predict the finite-length performance of spatially-coupled LDPC codes," *IEEE Trans. Inf. Theory*, vol. 61, no. 6, pp. 3164–3184, Jun. 2015.
[14] M. Stinner and P. M. Olmos, "On the waterfall performance of finite-length SC-LDPC codes constructed from protographs," *IEEE J. Sel. Areas Commun.*, vol. 34, no. 2, pp. 345–361, Feb. 2016.
[15] K. Liu, M. El-Khamy, and J. Lee, "Finite-length algebraic spatially-coupled quasi-cyclic LDPC codes," *IEEE J. Sel. Areas Commun.*, vol. 34, no. 2, pp. 329–344, Feb. 2016.

[16] Y. Liu, Y. Li, and Y. Chi, "Spatially coupled LDPC codes constructed by parallelly connecting multiple chains," *IEEE Commun. Lett.*, vol. 19, no. 9, pp. 1472–1475, Sep. 2015.
[17] Y. Fang, G. Bi, Y. L. Guan, and F. C. M. Lau, "A survey on protograph LDPC codes and their applications," *IEEE Commun. Surveys Tuts.*, vol. 17, no. 4, pp. 1989–2016, 4th Quart., 2015.
[18] P. Chen, L. Kong, Y. Fang, and L. Wang, "The design of protograph LDPC codes for 2-D magnetic recording channels," *IEEE Trans. Magn.*, vol. 51, no. 11, Nov. 2015, Art. no. 3101704.
[19] J. Thorpe, "Low-density parity-check (LDPC) codes constructed from protographs," in *Proc. IPN Progr. Rep.*, Aug. 2003, pp. 1–7.
[20] G. Liva and M. Chiani, "Protograph LDPC codes design based on EXIT analysis," in *Proc. IEEE GLOBECOM*, Nov. 2007, pp. 3250–3254.
[21] S. ten Brink, G. Kramer, and A. Ashikhmin, "Design of low-density parity-check codes for modulation and detection," *IEEE Trans. Commun.*, vol. 52, no. 4, pp. 670–678, Apr. 2004.
[22] S. Litsyn and V. Shevelev, "Distance distributions in ensembles of irregular low-density parity-check codes," *IEEE Trans. Inf. Theory*, vol. 49, no. 12, pp. 3140–3159, Dec. 2003.
[23] D. Divsalar, C. Jones, S. Dolinar, and J. Thorpe, "Protograph based LDPC codes with minimum distance linearly growing with block size," in *Proc. IEEE Global Commun. Conf.*, vol. 3, Nov. 2005, pp. 1–5.
[24] D. G. M. Mitchell, M. Lentmaier, and D. J. Costello, "On the minimum distance of generalized spatially coupled LDPC codes," in *Proc. IEEE ISIT*, Jul. 2013, pp. 1874–1878.

**ZHAOJIE YANG** received the B.Sc. degree in applied electronic technology from Lingnan Normal University, China, in 2016. He is currently pursuing the Ph.D. degree with the Department of Communication Engineering, Guangdong University of Technology, China. His primary research interest is channel coding.

**YI FANG** (M'15) received the B.Sc. degree in electronic engineering from East China Jiaotong University, China, in 2008, and the Ph.D. degree in communication engineering, Xiamen University, China, in 2013. In 2012, He was a Research Assistant in electronic and information engineering with The Hong Kong Polytechnic University, Hong Kong. From 2012 to 2013, he was a Visiting Scholar in electronic and electrical engineering with University College London, U.K. From 2014 to 2015, he was a Research Fellow with the School of Electrical and Electronic Engineering, Nanyang Technological University, Singapore. He is currently an Associate Professor with the School of Information Engineering, Guangdong University of Technology, China. His research interests include information and coding theory, LDPC/protograph codes, spread-spectrum modulation, and cooperative communications. He is an Associate Editor of the IEEE Access.

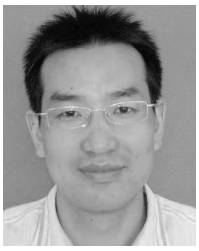

**GUOJUN HAN** (M'12–SM'14) received the M.E. degree in electronic engineering from the South China University of Technology, Guangzhou, China, and the Ph.D. degree from Sun Yat-sen University, Guangzhou. From 2011 to 2013, he was a Research Fellow with the School of Electrical and Electronic Engineering, Nanyang Technological University, Singapore. From 2013 to 2014, he was a Research Associate with the Department of Electrical and Electronic Engineering, The Hong Kong University of Science and Technology. He is currently a Full Professor and the Vice Dean with the School of Information Engineering, Guangdong University of Technology, Guangzhou. His research interests include wireless communications, coding, and signal processing for data storage.

**GUOFA CAI** (M'17) received the B.Sc. degree in communication engineering from Jimei University, Xiamen, China, in 2007, the M.Sc. degree in circuits and systems from Fuzhou University, Fuzhou, China, in 2012, and the Ph.D. degree in communication engineering from Xiamen University, Xiamen, in 2015. In 2017, he was a Research Fellow with the School of Electrical and Electronic Engineering, Nanyang Technological University, Singapore. He is currently an Associate Professor with the School of Information Engineering, Guangdong University of Technology, China. His primary research interests include information theory and coding, chaotic communications, and UWB communications.

**FRANCIS C. M. LAU** (M'93–SM'03) received the B.Eng. degree (Hons.) in electrical and electronic engineering and the Ph.D. degree from King's College London, University of London, U.K. He is currently a Professor and an Associate Head with the Department of Electronic and Information Engineering, The Hong Kong Polytechnic University, Hong Kong. He is a co-author of *Chaos-Based Digital Communication Systems* (Springer-Verlag, 2003) and *Digital Communications with Chaos: Multiple Access Techniques and Performance Evaluation* (Elsevier, 2007). He is also a co-holder of five U.S. patents. He has published over 280 papers. His main research interests include channel coding, cooperative networks, wireless sensor networks, chaos-based digital communications, applications of complex-network theories, and wireless communications. Prof. Lau is a fellow of IET. He was the Chair of the Technical Committee on Nonlinear Circuits and Systems, IEEE Circuits and Systems Society, in 2012–2013. He served as an Associate Editor for the IEEE Transactions on Circuits and Systems II in 2004–2005, the IEEE Transactions on Circuits and Systems I in 2006–2007, and the *IEEE Circuits and Systems Magazine* in 2012–2015. He has been a Guest Associate Editor of the *International Journal and Bifurcation and Chaos* since 2010 and an Associate Editor of the IEEE Transactions on Circuits and Systems II since 2016.